Bulletin of the Seismological Society of America, Vol. 103, No. 1, pp. 371–382, February 2013, doi: 10.1785/0120120076

Attenuation, Site Effects, and Source Parameters in the Three Gorges Reservoir Area, China

by Wei Hua, Sihua Zheng, Chunqing Yan, and Zhangli Chen

Abstract The temporal and spatial characteristics of 1924 post-impoundment earthquakes (M_L −0.3 to 3.1) recorded by 26 temporary stations from 16 March 2009 to 14 July 2010 in the Three Gorges reservoir area, Hubei Province, China, are investigated in this paper. The epicenters are mainly concentrated in three clusters and located along the Yangtze river within the range of 10 km from the reservoir waterfront. The hypocentral depths range from 0 to 15 km and appear to increase with the epicenters approaching the dam. Source parameters for 97 selected reservoir-induced earthquakes of $M_L \geq 1.5$ were estimated after applying corrections for geometrical spreading, frequency-dependent Q, and site effects. The results show that the seismic moments (M_0) are between 3.96×10^{11} and 4.07×10^{13} N · m, whereas static stress drops ($\Delta\sigma$) are 0.01–0.26 MPa. We find the static stress drops in this area vary with seismic moment for our data range, approximately as $\Delta\sigma \propto M_0^{0.46}$. Apparent stresses we obtained lie between 0.0019 and 0.049 MPa and also increase with increasing seismic moment, indicating that large earthquakes radiate more energy per seismic moment than smaller ones in the Three Gorges reservoir area and do so more efficiently. Our results show that reservoir-induced earthquakes appear to have systematically lower stress drop with respect to natural tectonic earthquakes, by about one order of magnitude. This may be attributed to the high pore pressures of the underground medium, and the presence of water decreasing the coefficient of friction.

Introduction

The scaling of earthquake-source parameters with magnitude has been a point of debate in recent years. This debate is motivated by the implications for understanding earthquake-source physics. The issue is whether large earthquakes can be adequately approximated by linearly scaling the attributes of smaller earthquakes or something fundamentally differs in the rupture physics of different-size earthquakes (Kane *et al.*, 2011). Many results have shown that seismic moment is proportional to the source dimension cubed over a wide range of magnitudes (∼0–7), corresponding to the stress drop being independent of magnitude (Scholz, 1990; Abercrombie and Leary, 1993; Abercrombie, 1995; Kanamori and Brodsky, 2004; Allmann and Shearer, 2007, 2009). However, a number of studies have found a breakdown in self-similarity and stress drop appears to decrease with decreasing seismic moment (Dysart *et al.*, 1988; Mayeda and Walter, 1996; Hardebeck and Hauksson, 1997; Mandal *et al.*, 1998; Tusa and Gresta, 2008; Mandal and Dutta, 2011), especially for the small earthquakes ($M \leq 3$). Therefore, source parameters of small earthquakes are important for clarifying the scaling relations of earthquakes and understanding the differences between how small and large earthquakes dynamically rupture. Because of the difficulties in recording the high-frequency content of small earthquakes, it is often difficult to accurately determine source parameters of the small earthquakes (Yamada *et al.*, 2005). Empirical Green's functions (EGF) method (Hartzell, 1978; Frankel and Kanamori, 1983; Mori and Frankel, 1990; Mori, 1993) was considered to be a perfect method to remove the attenuation along the path and site effects from the record, but many studies still applied corrections for path and site effects individually (Atkinson and Mereu, 1992; Moya *et al.*, 2000; Zhao *et al.*, 2011), as the number of earthquakes for which source parameters could be obtained by the EGF method are limited (Tomic *et al.*, 2009) and the stress drops produced from them may be higher than the typically used single event spectral analysis (Ide *et al.*, 2003).

Seismicity associated with reservoir impoundment and seasonal variation in water level is termed reservoir-induced seismicity (RIS), and is a well-accepted phenomenon (Gupta, 1992; Talwani, 1997a,b; Tomic *et al.*, 2009). Roeloffs (1988) and Simpson *et al.* (1988) have suggested how some reservoirs can induce or trigger earthquakes immediately upon filling due to elastic stress changes and after a delay as a result of pore pressure and fluid diffusion. Many studies have discussed the difference between the RIS and natural tectonic

earthquakes, especially with the development of digital observation techniques. For example, some studies have indicated that RIS has significant non-double-couple components in its source mechanism (Ross *et al.*, 1999) and smaller stress drop, compared with the same size natural tectonic earthquake (Fehler and Phillips, 1991; Gibowicz *et al.*, 1991; Abercrombie and Leary, 1993; Mandal *et al.*, 1998). In addition, some results show that there are some differences in the source spectrum between them (Zhou *et al.*, 2006).

The Three Gorges Project (TGP), which is located on the Yangtze river in Hubei Province, China (Fig. 1), is a world-famous hydropower and water conservancy project in China. Despite the benefits of the 181-m-tall dam in terms of power generation and flood control, the TGP has attracted attention for its potential impact on earthquakes, ecosystems, and geohazards. The Three Gorges reservoir began the first filling in June 2003. The number of earthquakes per month from 2000 to 14 July 2010 shows the rapid increase of seismicity in the Three Gorges reservoir after the impoundment. More than 2000 microearthquakes abruptly occurred along the river in Badong county of Hubei Province beginning on 7 June 2003, and attracted great attention (Li *et al.*, 2005). Seismotectonic analysis of the distribution of several active faults and their intersections and seismogenic capacity in the eastern part of the Three Gorges reservoir area suggested that two potential seismic focus zones located in Badong and Xiangxi may be hit by a reservoir-induced earthquake of upper-limit magnitude about 5.5 (Li *et al.*, 2005).

The National Key Technology Research and Development (R&D) Program monitoring and Research Technology of Reservoir Earthquakes (2008BAC38B02) carried out temporary monitoring for about one year in the Three Gorges reservoir, the Longtan reservoir, and the Xinfengjiang reservoir, respectively, beginning in March 2009. In this paper, we first investigate the characteristics of seismic events recorded by the temporary stations in the Three Gorges reservoir. Then, we estimate the source parameters such as seismic moment (M_0), static stress drop ($\Delta\sigma$), and apparent stress (σ_a) for these events after applying corrections for geometrical spreading, frequency-dependent Q, and site effects. Finally, we discuss the differences of source parameter characteristics between RIS and natural tectonic earthquakes.

Geological Setting in the Three Gorges Reservoir

The Three Gorges reservoir is located in western Hubei, part of South China's weak seismicity region. It is mainly supplied by the Yangtze, Jiuwanxi, Xiangxi, Shuitianba, Tongzhuang, Qinggan, and Yandu rivers, and the dam is

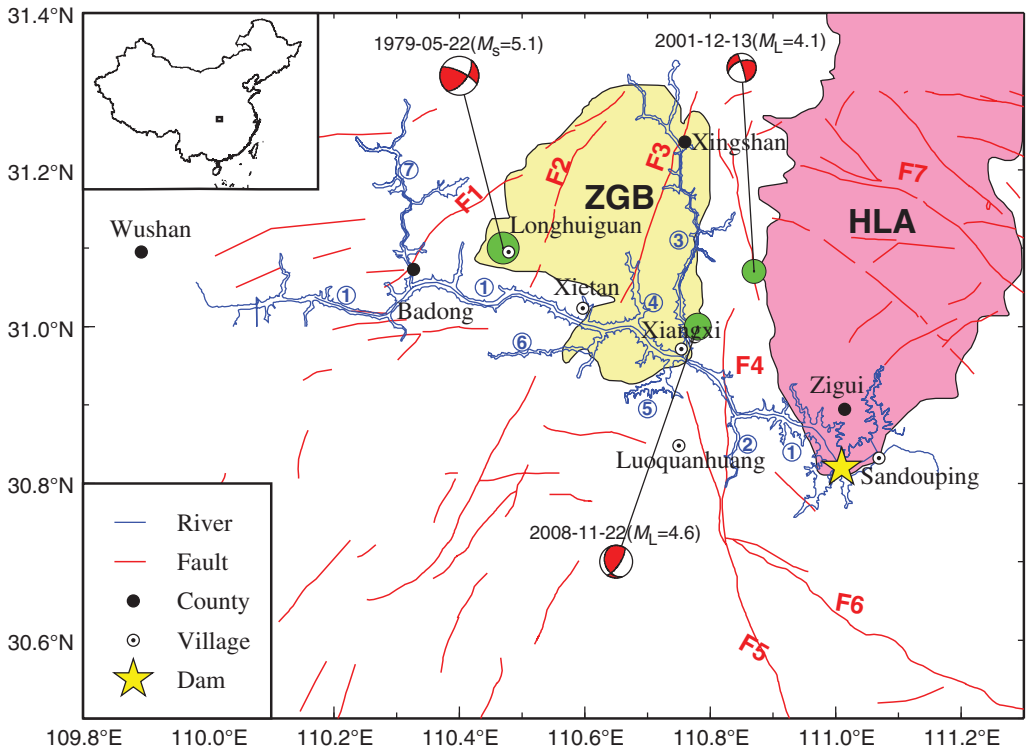

Figure 1. Map showing geologic structure in the Three Gorges reservoir area. The primary character of geological setting in the studied area consists of Zigui basin (ZGB) and Huangling anticline (HLA). The faults names are as follows: F1 Gaoqiao fault; F2 Niukou fault; F3 Shuitianba fault; F4 Jiuwanxi fault; F5 Xiannvshan fault; F6 Tianyangping fault; F7 Wuduhe fault. The Three Gorges reservoir is mainly supplied by the 1, Yangtze river; 2, Jiuwanxi river; 3, Xiangxi river; 4, Shuitianba river; 5, Tongzhuang river; 6, Qinggan river; 7, Yandu river. The small map in the upper left corner is an index map to show the location of our study area. Focal mechanisms of three important earthquakes shown by green circles are given.

located southeast of the reservoir. The primary character of the geological setting in the Three Gorges reservoir region (109.8° E–111.3° E, 30.5° N–31.4° N) consists of Zigui basin (ZGB) and Huangling anticline (HLA) (Fig. 1; Li *et al.*, 2009). There are seven major faults surrounding the two tectonic units in the reservoir area, the northeast-trending Gaoqiao fault (F1), the north-northeast-trending Niukou fault (F2), the northeast-trending Xingshan–Shuitianba fault (F3), and the northwest-trending Wuduhe faults (F7). The north-northeast-trending Jiuwanxi fault (F4) is located southwest of HLA and consists of two parallel diagonals, with an interval of 1 km. The north-northwest-trending Xiannvshan fault zone (F5) is located southwest of HLA, about 19 km from the dam. It is about 100-km long and consists mainly of breccia and clastic rock. The northwest-trending Tianyangping (F6) is located north of Changyang anticline, about 60 km, and its west segment is cut off by the Xiannvshan fault. In the Zigui basin, clastic sandy shale is deposited, and the Huangling anticline mainly formed from the crystallization rocks of granite, whereas in the surroundings of Zigui basin and Huangling anticline is an area of limestone (Ma *et al.*, 2011). The Jiuwanxi fault (F4) and its adjacent regions between the Huangling anticline and the Zigui basin form the contact between granite and carbonate rocks (Li *et al.*, 2009).

Seismic Monitoring and Seismicity in the Three Gorges Reservoir

A few tectonic earthquakes occurred in the Three Gorges reservoir area before reservoir construction. About 300 earthquakes were recorded from 143 B.C. to 1959, within a radius of 300 km from the dam, and 47 of them were large earthquakes ($M \geq 4.7$). A seismic analog network had been built since September 1959 and the detection thresholds in this region could reach M_L 1.5 (Yang and Zhang, 2001). The maximum magnitude of tectonic earthquake was an M_S 5.1 earthquake that occurred 22 May 1979 in Longhuiguan, Zigui (Fig. 1). The reconstructive seismic analog network, which was composed of eight stations, was put into operation in 1997 and the detection thresholds in this region improved to reach M_L 1.0 (Yang and Zhang, 2001). Under the effect of the regional tectonic stress field, earthquakes in the Three Gorges reservoir area mainly related to the north-northwest-trending Xiannvshan fault (F5), the north-northeast-trending Xinghua fault, the Jiuwanxi fault (F4), and the northeast-trending Gaoqiao fault (F1; Li *et al.*, 2009). HuBei Three Gorges Reservoir Digital Seismic Station Network (HBTGRDSSN) has been in operation since July 2001 to monitor the seismicity in the Three Gorges reservoir area. It is composed of 24 digital permanent seismic stations that are located mainly in the Hubei province segment of Three Gorges reservoir, from Badong county to Sandouping where the dam is located (Wang, 2009). Twenty of these stations are 16-bit EDAS data recorders and the other four stations are 24-bit EDAS data recorders. All seismograms are sampled at a rate of 100 samples per second (Liao *et al.*, 2009). The average distance among these stations is about 15–20 km and the detection thresholds in this region can reach M_L 0.5 (Li *et al.*, 2009). HBTGRDSSN recorded all earthquakes prior and post the impoundment that began on 1 June 2003. More than 250 earthquakes were recorded by HBTGRDSSN before the impoundment and the biggest earthquake was the M_L 4.1 that occurred on 13 December 2001 in Zigui (Fig. 1).

There were three water-filling periods in the Three Gorges reservoir (Fig. 2). The water level (the depth of water near the dam) was about 80 m in May 2003. The first filling began on 1 June 2003. A rise in water level of 40 m took place in 10 days, and the water level reached 135 m. The second filling took place from 20 September 2006 to 27 October 2006, and the water level reached 156 m. The third filling began in September 2008 and the water level reached the maximum value (175 m) (Wang, 2009). Since the impounding of Three Gorges reservoir on 1 June 2003, seismic activity has increased significantly. The monthly frequency of earthquakes on average reaches 40 or so, and the seismicity has had an obvious correlation with water-level changes. During the process of reservoir water-level decrease, relatively fewer earthquakes occur in the reservoir area; whereas during increase, the earthquake frequency in the reservoir area increases comparatively (Ma *et al.*, 2011). Earthquakes have been mainly concentrated in three clusters, namely the north end of the Xiannvshan fault, the Gaoqiao fault zone, and to the west of Xietan township (Liao *et al.*, 2009). The maximum magnitude of post-impoundment events was an M_L 4.6 that occurred on 22 November 2008 in Quyuan township, Zigui (Fig. 1). The reservoir-induced earthquakes are attributed to the activities related to loading of the reservoir in the Xiannvshan fault zone, the Gaoqiao fault zone, and the Niukou fault (Ma *et al.*, 2011).

Funded by the National Key Technology R&D Program, we set up a Portable Digital Seismic Station Network (PDSSN) in the Three Gorges reservoir in March 2009 which

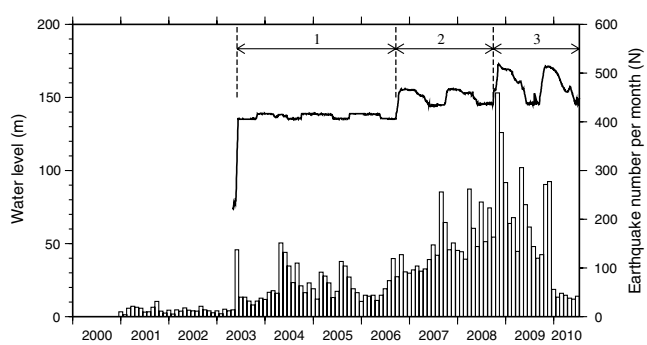

Figure 2. Relation between water level (the depth of water near the dam) and seismicity in the Three Gorges reservoir. Three water-filling periods are shown by vertical broken lines in the Three Gorges reservoir. The number of earthquakes per month from 2000 to 14 July 2010 shows the rapid increase of seismicity in the Three Gorges reservoir after the impoundment.

was composed of 26 stations. All of the PDSSN stations were equipped with three-component velocity seismometers. Twenty-two of them were equipped with L-22 E/3D short-period seismometers and REFTEK130B data recorders with 200 samples per second. The other four stations were equipped with GuralpCMG-3ESPC broadband seismometers with 60 s–50 Hz frequency range and REFTEK130B data recorders with 100 samples per second.

About 1924 seismic events with M_L $-0.3 \sim 3.1$ occurring in the Hubei section of the Three Gorges reservoir region were detected by PDSSN from 16 March 2009 to 14 July 2010 (Fig. 3). The number of events of $M_L < 0$ is 16, that of M_L $0 \sim 0.9$ is 1580, that of M_L $1.0 \sim 1.9$ is 286, that of M_L $2.0 \sim 2.9$ is 41, and that of $M_L \geq 3.0$ is 1. The maximum magnitude of these events was an M_L 3.1 that occurred on 29 April 2010. The characteristics of the epicentral distribution and hypocentral depth are similar to that suggested by Liao *et al.* (2009), which were based on the data from 2001 to 2007. Seismic events were also mainly concentrated in three clusters, namely the Gaoqiao fault zone (A cluster), the west of Xietan township (B cluster), and the north end of the Xiannvshan fault (C cluster). The hypocentral depths of these 1924 events range from 0 to 15 km, mainly smaller than 7 km. Furthermore, along the latitude direction, the hypocentral depths appear to increase from west to east. The observation of deeper earthquakes closer to the dam (greater water depth) is interesting. However, for these earthquakes in cluster C that exhibit greater depth, the temporal variance of the depth shows that the hypocentral depths appear to decrease during the period from March 2009 to July 2010.

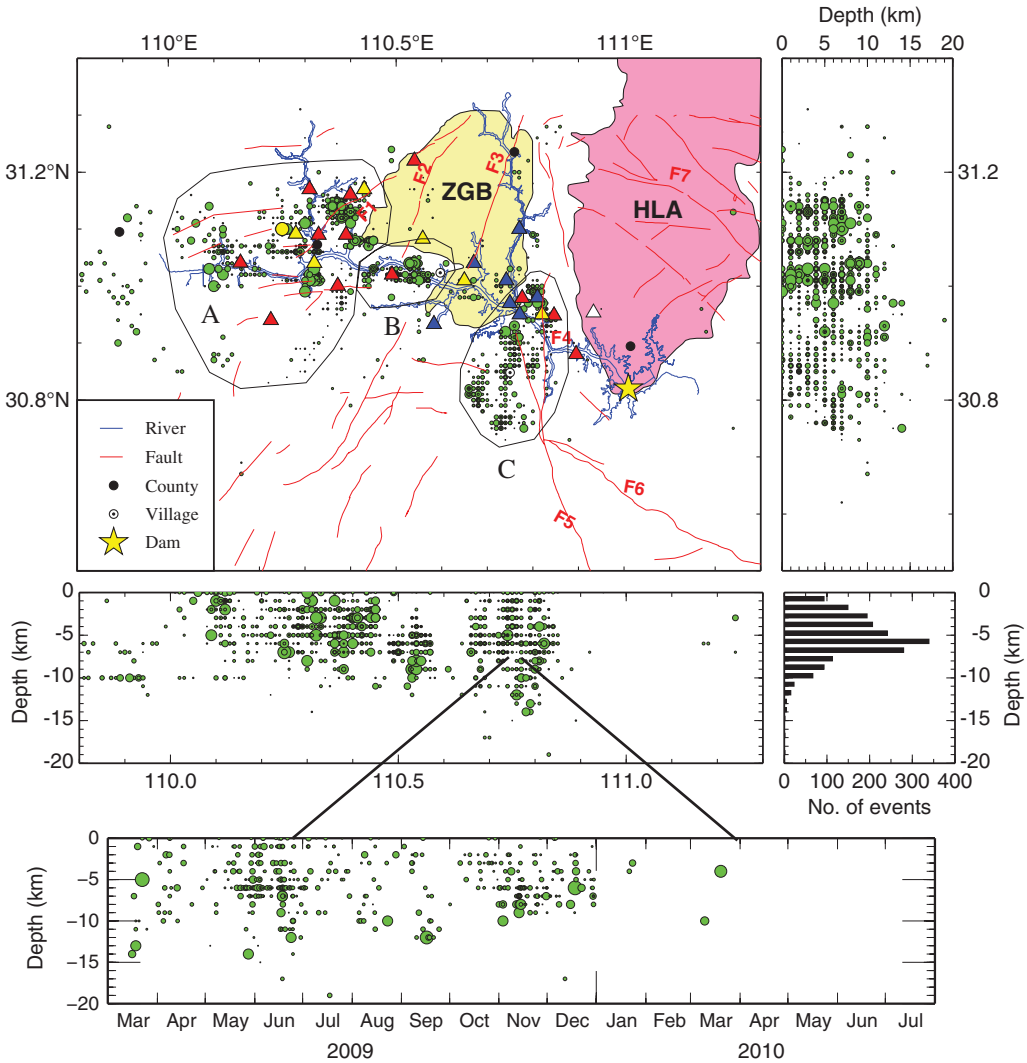

Figure 3. The distribution of the events (green circles) and stations (triangles) in the Three Gorges reservoir. These earthquakes are mainly distributed in three clusters (labeled by black curves). The yellow circle corresponds to the biggest event with M_L 3.1 that occurred on 29 April 2010. The rock lithologies of all stations are shown with different color triangles: red, blue, yellow, and white triangles correspond to limestone, sandstone, shale, and granite, respectively. The temporal variance of the depth only for those earthquakes in cluster C is shown by the bottom sketch map.

Determination of Source Parameters

The seismic source effect of the ith earthquake $S(f)_i$ can be represented as the multiplication of several physical parameters in frequency domain (Iwata and Irikura, 1988; Moya *et al.*, 2000):

$$S(f)_i = O(f)_{ij} R_{ij} e^{\pi R_{ij} f / Q(f) V_S} G^{-1}(f)_j, \tag{1}$$

for which $O(f)_{ij}$ is the observed displacement spectrum for the ith earthquake observed at the jth receiver, R_{ij} is the hypocentral distance from the ith source to the jth receiver, $Q(f)$ is the quality factor, V_S is the S-wave velocity of the medium, and $G(f)_j$ is the site effect of the jth receiver.

In order to recover the source spectrum $S(f)$, the observed waveform must be corrected for the propagation path and site effect. Following the method of Atkinson and Mereu (1992), we calculate the quality factor Q value by using the multiple stations and source joint inversion (Huang *et al.*, 2003; Liu *et al.*, 2003; Hua *et al.*, 2009). Meanwhile, we estimate the site effect by using the same multiple stations and source joint inversion following the method proposed by Moya *et al.* (2000).

The source-displacement spectrum after removing the effects due to the attenuation along the path and site effect from observational spectra is termed actual spectra in this paper. It was then fitted by the Brune model (Brune, 1970, 1971) based on genetic algorithms (GA) arithmetic (Holland, 1975). We called the fitting spectra model spectra, to obtain the source-spectra parameters: the source-spectrum flat levels Ω_0 and the corner frequency f_c. Finally, source parameters such as seismic moment (M_0) and the static stress drop ($\Delta\sigma$) are calculated from Ω_0 and f_c by using the following equations:

$$S(f) = \frac{\Omega_0}{1 + (f/f_c)^2}, \tag{2}$$

$$M_0 = \frac{4\pi\rho V_S^3 \Omega_0}{R_{\theta\varphi}}, \tag{3}$$

and

$$\Delta\sigma = k M_0 f_c^3, \tag{4}$$

for which $k = (7/16) \times (2\pi/2.34V_S)^3$, the material density ($\rho$) is taken to be 2700 kg/m^3, S-wave velocity (V_S) is taken to be 3.5 km/s. To account for the free surface effect precisely, only SH waves are used in our paper (free surface effect is 2) and the average radiation pattern ($R_{\theta\varphi}$) is taken to be 0.41 for SH (Stork and Ito, 2004).

After having obtained the source-displacement spectra, we can calculate the radiated seismic energy E_R and apparent stress ($\sigma_a = \mu E_R / M_0$; Wyss and Brune, 1968), for which μ is the rigidity. As the S wave is the dominant component in the energy radiated from the hypocenter, we approximate the radiated energy using only the S-wave energy. Radiated energy of a far field can be expressed as follows in the frequency domain (Izutani and Kanamori, 2001):

$$E_R = \frac{4\pi}{5\rho V_S^5} \int \left| f \frac{M_0}{1 + (f/f_c)^2} \right|^2 df. \tag{5}$$

Ide and Beroza (2001) argued that limited bandwidth recording and the uncertain adjustment of seismic attenuation along the wave path can lead to substantial underestimation of the radiated seismic energy. The question appears to be more critical for small earthquakes because they contain more high-frequency components and their corner frequency is larger than that of larger earthquakes. According to Ide and Beroza (2001), integration up to approximately ten times the corner frequency is necessary to approach 90% of the seismic energy. This condition is not often met for seismic observations because of limited bandpass in the recording seismometers and attenuation that decreases the amplitude at high frequencies. In this paper, in order to include sufficiently high frequencies when calculating the radiated energy, we compute energy from the best fitting model spectra by extending the upper integration limit to ten times the corner frequency of the event we studied, rather than directly from the actual spectra mentioned previously in this paper (Prieto *et al.*, 2004).

Data Processing

The data-processing techniques applied here are similar to that defined by Atkinson and Mereu (1992). For each record we determine the S window as that which begins with the first discernible S arrival and continues until approximately 90% of the total S energy has been accumulated (as indicated by the cumulative square of the velocity; Fig. 4a). The S window includes the direct arrival for near distances. At greater distances, it also includes reflections from internal crustal interfaces and the Moho discontinuity. Following Chael (1987), we use a lag-window spectral technique to obtain stable estimates of the Fourier spectrum. The S window is subdivided into some segments; each segment length is about 5.12 s in duration, with 50% overlap between segments. For each segment, a 5% cosine-taper is applied to both ends of the time series and the spectrum is obtained by fast Fourier transform. The noise was estimated from a one-segment time interval (5.12 s) immediately preceding the P-wave arrival, processed in the same way as the signal (Fig. 4a). As four of our 26 stations were equipped with REFTEK130B data recorders with 100 samples per second, the highest frequency we analyzed was set to be 40 Hz. Accordingly, to assure the resolution of the true corner frequency, only earthquakes with $M_L \geq 1.5$ were selected for estimation of source parameters. We require a minimum mean signal-to-noise ratio (SNR) of 1.5 as measured over bandwidths below 40 Hz (Fig. 4b). Events with fewer than three stations meeting SNR requirements are excluded from further analyses.

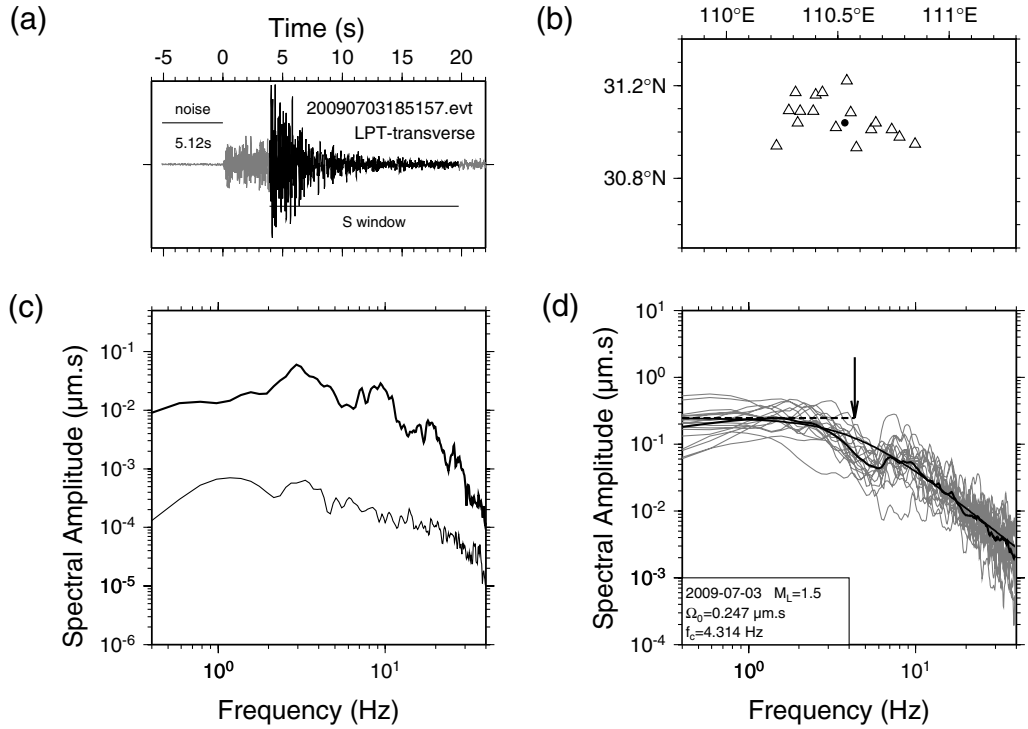

Figure 4. (a) Example seismogram for an event of M_L 1.5 recorded at station LPT, transverse component. Horizontal bars represent *S* window as defined by the 90% energy criterion and noise. (b) The distribution of stations that recorded this event. (c) The thick black curve depicts Fourier spectra for *SH* displacement and the thin gray curve represents noise. Only the records with a signal-to-noise ratio bigger than 1.5 over bandwidths below 40 Hz were included for further analysis. (d) Gray lines denote the results obtained by each station, and the thick irregular curve denotes the average (we call it actual spectra in this paper). The smooth curve denotes source spectra obtained by GA inversion based on the Brune model (we call it model spectra in this paper). This smooth curve will be used to estimate the energy rather than the thick irregular curve. Source parameters for this event are shown at the bottom-left corner. The dashed line shows the zero-frequency level and the arrow shows the corner frequency.

As a result, the quality factor we obtained for the Three Gorges reservoir region is$Q(f) = 112.0f^{0.918}$, and site effects for 25 stations were also obtained (Fig. 5), following the method proposed by Moya *et al.* (2000). According to the rock lithology (Ma *et al.*, 2011), there are four kinds of basement rocks for these stations. Among these, 11 stations are limestone, 7 stations are sandstone, 6 stations are shale, and 1 station (TPX) is granite (Fig. 3). Most of these site effects are between 1 and 10, except for stations JWX, PYB, SBC, and YDB. The basement rocks of the four stations with relatively high amplifications are limestone, whereas that of other stations are sandstone or shale. There are some differences in site effects among these stations with different basement rock (Fig. 5). Site effects of seven stations located on sandstone sites have the same characteristics except for TDH station. There is amplification from 1 to 5 Hz and deep decay for frequencies higher than around 5 Hz in these six stations. For stations located on shale basement rock, site effects are similar to that of stations located on sandstone basement rock. In contrast, site effects for limestone basement-rock stations show that the amplification almost exists in the entire frequency range of interest. We also note that site effect at TPX located on granite is flat up to approximately 4.5 Hz and there is significant amplification for frequencies higher than 4.5 Hz. The amplitude of the low frequency of the site effect at TPX is about two. This is theoretically acceptable for a rock site in the low-frequency range (Moya *et al.*, 2000). Site effect is usually estimated by dividing the observed spectra at the sediment sites by those at the rock sites (Borcherdt, 1970). This technique works under the assumption that the site effect of rock sites is flat in the frequency range of interest. However, our results show that assumption does not hold for TPX. In addition, a relative estimate would introduce serious bias by the choice of reference station (Moya *et al.*, 2000).

Resulting Scaling Relations

Following the same data-selecting rule that an earthquake must be recorded by at least three stations, one station must record at least three earthquakes, and the SNR is greater than 1.5 over bandwidths below 40 Hz, from 1924 earthquakes recorded in the Three Gorges reservoir area, source parameters of 97 selected earthquakes with $M_L \geq 1.5$ were calculated in this paper. The seismic moments of our results are between 3.96×10^{11} and 4.07×10^{13} N · m. Figure 6a shows that there is a strong linear correlation between seismic moment and magnitude with $\log M_0 = 1.14M_L + 10.15$, and

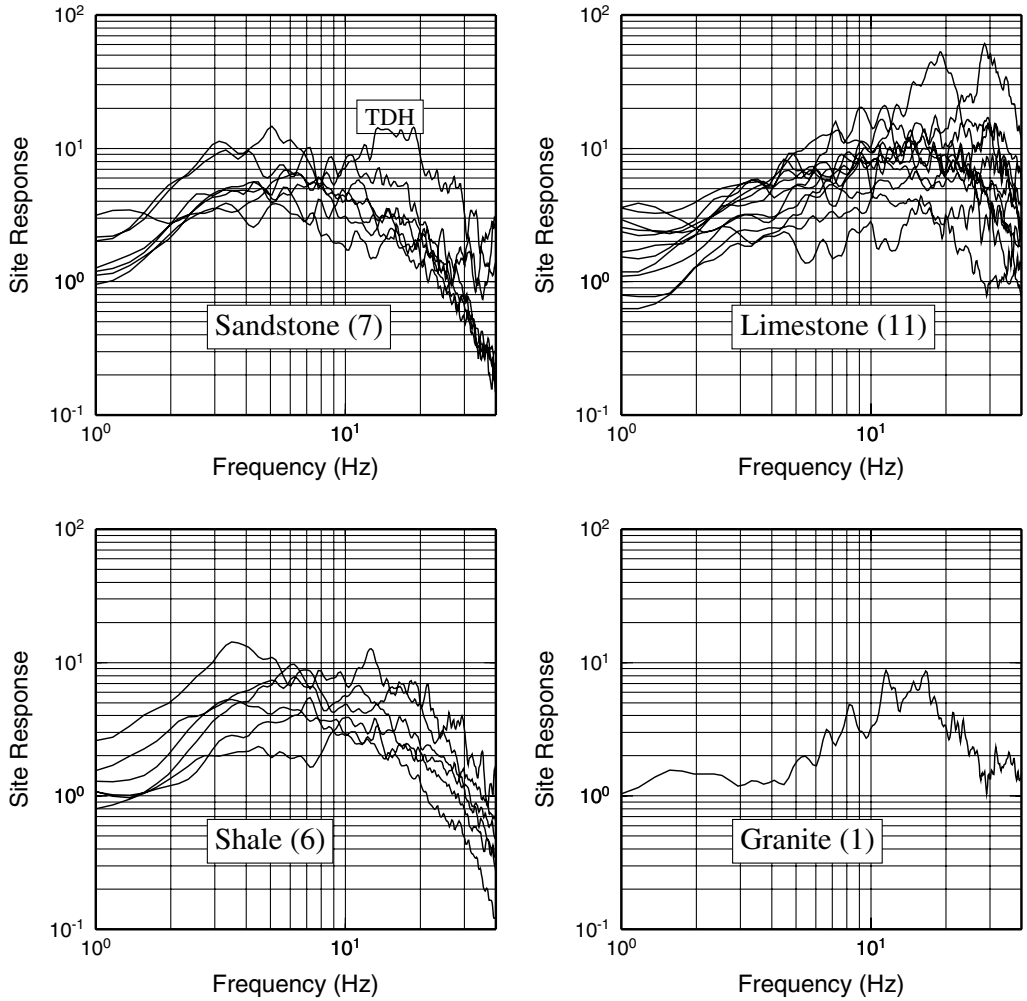

Figure 5. Comparison of site effects for 25 stations with different rock lithology in the Three Gorges reservoir. The rock lithologies are labeled together with the number of stations.

the correlation coefficient is 0.93. The plot of M_0 versus f_c is shown in Figure 6b. A regression analysis yields $\log M_0 = -3.44 \log f_c + 14.61$ and the correlation coefficient is 0.79. There is slight difference in the $M_0 - f_c$ relation obtained in this paper ($M_0 \propto f_c^{-3.44}$) and the constant stress drop scaling ($M_0 \propto f_c^{-3.0}$). Stress drops obtained in our paper are mainly between 0.01 and 0.26 MPa and Figure 6c shows that stress drop increases with increasing seismic moment. The correlation coefficient is 0.73 and the corresponding relation is $\log \Delta\sigma = 0.46 \log M_0 - 7.02$.

Estimates of apparent stress σ_a have been preferred to stress drop in some studies (e.g., Snoke *et al.*, 1983; Houston, 1990) on account of the large errors associated with stress-drop measurement. Our results show that apparent stresses are between 0.0019 and 0.049 MPa and also vary with seismic moment (Fig. 6d). As shown in Figure 6, there is a strong relationship between Brune static stress drop and apparent stress in the Three Gorges reservoir. Their relation ($\sigma_a = 0.19\Delta\sigma$) is close to the theoretical relationship ($\sigma_a = 0.23\Delta\sigma$; Singh and Ordaz, 1994) and the ratio of apparent stress to stress drop does not vary with seismic moment.

Discussion

Factors that control RIS include the size of the reservoir and nature of lake level changes, pre-existing faults, ambient state of stress, availability and interconnectedness of fractures and hydromechanical properties of the underlying rocks (Bell and Nur, 1978; Roeloffs, 1988; Talwani, 1997a). There was a rapid increase of earthquakes after the impoundment in June 2003 in the Three Gorges reservoir region and the seismicity had an obvious correlation with water-level changes, suggesting the seismicity was reservoir induced. Figure 3 shows that the 1924 seismic events recorded by PDSSN in the Three Gorges reservoir region from 16 March 2009 to 14 July 2010 were mainly concentrated in three clusters. That the distribution appear to be clustered distribution rather than along the direction of faults suggests the reservoir-induced earthquakes in the Three Gorges reservoir region are not controlled by fractures and these faults intersecting

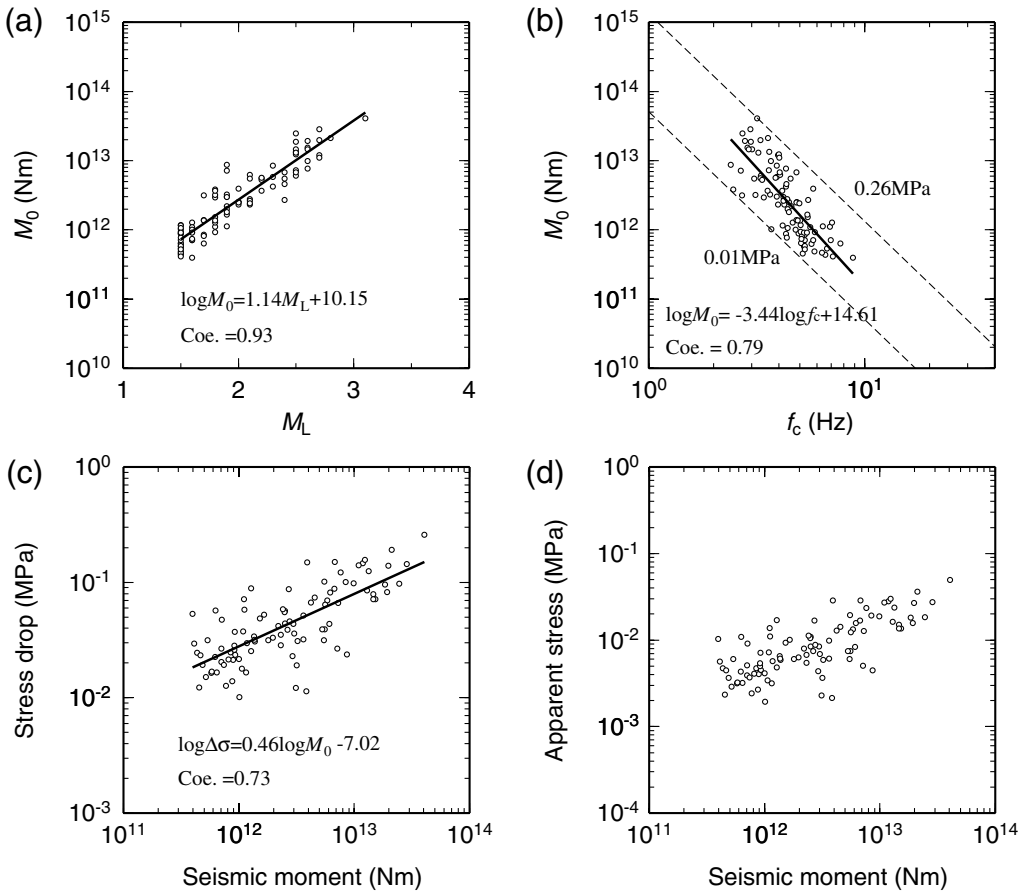

Figure 6. Scaling relations of source parameters in the Three Gorges reservoir. (a) Seismic moment and magnitude. (b) Seismic moment and corner frequency. (c) Stress drop and seismic moment. (d) Apparent stress and seismic moment.

the reservoir, which appear to just serve as conduits for flow away from the reservoir. There is some relationship between the water depth and the hypocentral depths for the 1924 earthquakes, but their depths are shallow in general (mainly smaller than 7 km). Meanwhile, the hypocenters of these events are closer to the main rivers, within the range of 10 km from reservoir waterfront, demonstrating that the earthquakes near the main rivers may be caused by water loading and unloading of the reservoir and the water influence may be restricted to a small region, whether in the horizontal or in the vertical direction. In addition, it is worth noting that few earthquakes occurred to the east of the Jiuwanxi fault (F4) and the smallest distance to the dam is larger than ~20 km, indicating the complicated factors contributed to the RIS in the Three Gorges reservoir region.

For earthquakes above M_w 3, it has long been known that stress drop does not vary systematically with earthquake size. This results in the well-known scaling relationships of characteristic length and time with seismic moment (e.g., Kanamori and Anderson, 1975; Hanks, 1977). However, several studies have suggested that the scaling of small earthquakes is different from that of larger events (Archuleta *et al.*, 1982; Archuleta, 1986). Nuttli (1983) concluded that the scaling relations developed for mid-plate earthquakes differ from those of plate-margin events. Our results are consistent with the mid-plate earthquake with increasing stress-drop model proposed by Nuttli (1983) and the results for other mid-plate-event studies obtained by Dysart *et al.* (1988) and Mandal *et al.* (1998). The relation between static stress drop and seismic moment is complicated due to the large errors associated with static stress-drop determinations (from the dependence on the cube of the corner frequency). The rupture speed may be another important source parameter for investigating the scaling of small to large earthquakes (Kanamori and Rivera, 2004; Yamada *et al.*, 2005; Tomic *et al.*, 2009). It is difficult to measure rupture velocity of small earthquakes due to the attenuation of high-frequency energy, and poor azimuthal coverage of recordings. Frankel and Kanamori (1983) demonstrated that small ($M < 2.5$) earthquake pulse widths are dominated by path effects even for short source-to-receiver distances (<40 km). Many ideas have been proposed for reducing the uncertainty in static stress-drop determinations (Andrews, 1986; Snoke, 1987; Di Bona and Rovelli, 1988; Prieto *et al.*, 2004; Shearer *et al.*, 2006), but errors of over a factor of ten (the typically quoted error) are likely. In this paper, however, the chief results are based on the data set as a whole, the area of seismic moment space occupied by the entire data set is considerably better constrained, and the

average value of the static stress drop for each seismic moment is reliable.

Basically, constant E_R/M_0 scaling implies similar physics for both small and large events. On the other hand, increasing E_R/M_0 scaling with moment implies that large events are more efficient radiators of seismic energy than small ones. Ide and Beroza (2001) believed that trends of increasing apparent stress with moment, at least in some studies, are artifacts due to measurement or analysis errors associated with estimating radiated energy. Bandwidth limitations can lead to underestimated radiated energy, particularly for small earthquakes (Ide and Beroza, 2001) that can have corner frequencies of the same order as the maximum observable frequency. However, our results show that apparent stress still increases with increasing seismic moment after already accounting for the missing energy, indicating large earthquakes radiated more energy per seismic moment than small earthquakes in the Three Gorges reservoir. Many other studies find the same results (Kikuchi and Fukao, 1988; Kanamori *et al.*, 1993; Singh and Ordaz, 1994; Abercrombie, 1995; Mayeda and Walter, 1996; Perez-Campos and Beroza, 2001; Prejean and Ellsworth, 2001). One can imagine a variety of mechanisms that might lead to this behavior (Kanamori and Brodsky, 2004). For example, if the dynamic or sliding friction were to decrease as earthquake size increased it could cause this effect. There has been a lot of work in earthquake physics looking at the idea of velocity or slip weakening, that is, as sliding begins it causes the friction to decrease, leading to further sliding and an earthquake. For RIS, fluid pressurization (e.g. Sibson, 1973) and elastohydrodynamic lubrication (Brodsky and Kanamori, 2001) will accelerate the decreasing course of the dynamic or sliding friction (Walter *et al.*, 2006).

It is interesting to study the discriminatory characteristics that differentiate RIS from the normal tectonic earthquakes (Gupta *et al.*, 1972a,b). Many earlier studies have suggested that hydrofractures, mining, and reservoir-induced earthquakes have lower average stress drop than natural tectonic earthquakes (Fehler and Phillips, 1991; Abercrombie and Leary, 1993; McGarr, 1993). Figure 7 compares our result with earlier studies of scaling parameters (Archuleta *et al.*, 1982; Mori and Frankel, 1990; Boatwright, 1994; Humphrey and Anderson, 1994; Abercrombie, 1995; Hough, 1996; Tajima and Tajima, 2007; Allmann and Shearer, 2009; Zhao *et al.*, 2011). The source parameters of about 2573 natural tectonic events of $3.0 \le M_L \le 6.0$ from 2001 to 2010 that occurred mainly in seismically active regions of mainland China, were estimated by Zhao *et al.* (2011) using

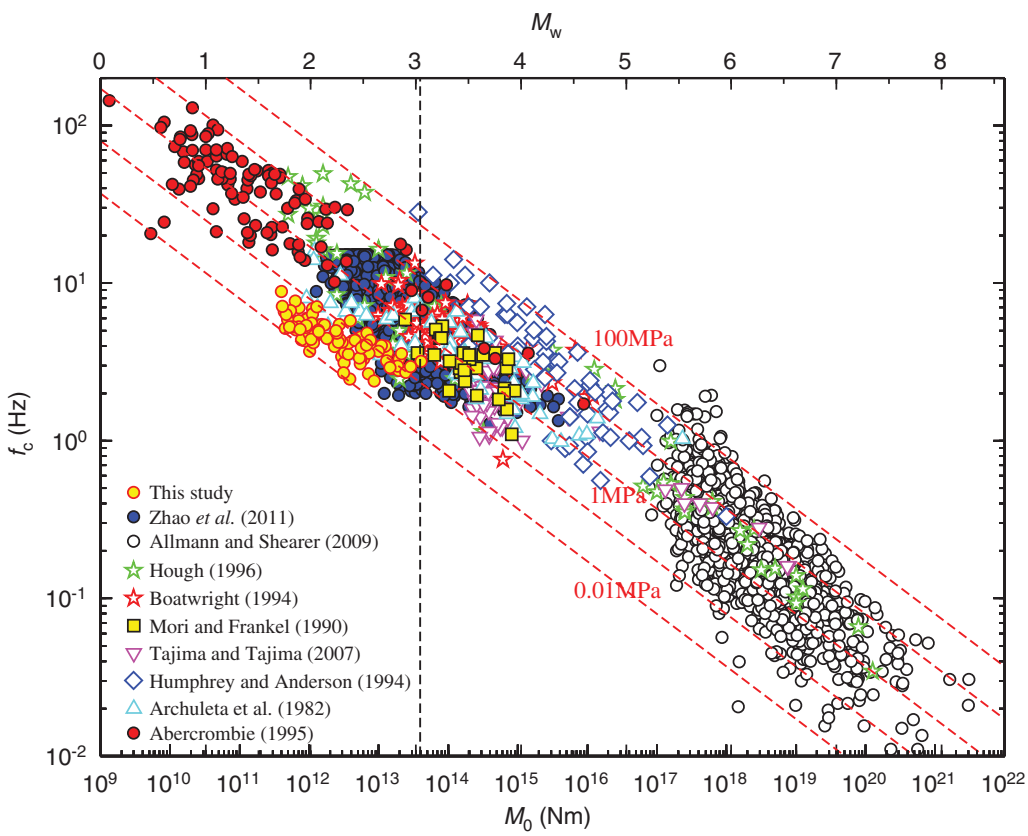

Figure 7. Corner frequency versus seismic moment (lower scale) and moment magnitude (upper scale). The dashed lines show constant stress drops of 0.01, 0.1, 1, 10, and 100 MPa. The vertical dashed line marks the higher magnitude cutoff of our data. The results of this paper are plotted as solid yellow circles. All other differently shaped symbols show data from various other studies collected by Allmann and Shearer (2009) and Zhao *et al.* (2011).

the same procedure applied in our paper. These other earlier studies of scaling parameters were collected by Allmann and Shearer (2009). Figure 7 shows that the result proposed by Zhao *et al.* (2011) is consistent with the other natural tectonic results, indicating that the same procedure applied in our paper is reasonable. The compilation results show that RIS in the Three Gorges reservoir appears to have lower corner frequency with respect to the tectonic earthquake and the stress drops of RIS are significantly lower than the tectonic earthquake, by at least a factor of ten.

We noted that Tomic *et al.* (2009) estimated recently a stress drop of about 26–179 MPa for six RIS events with $1.9 \leq M_L \leq 2.1$ in the Acu reservoir, northeast Brazil, and found them to be similar to, or higher than, those of large, natural earthquakes. We guess it may due to the assumptions that they used, such as frequency-independent Q, a dynamic source model rather than the Brune model, in which stress drops are closer to the absolute values and more consistent with frictional failure. In addition, the phenomenon that the EGF method produced higher stress-drop values than the typically used single-event spectral analysis found by Ide *et al.* (2003) deserves to be considered.

The filling of large reservoirs modifies the tectonic stress regime, either by increasing the vertical stress through the effect of loading or by increasing the pore pressure, which results in a decrease in the effective normal stress (Snow, 1972; Bell and Nur, 1978; Roeloffs, 1988). The hypocentral depths of these 97 selected earthquakes with $M_L \geq 1.5$ in our paper are mainly smaller than 7 km, but we cannot completely attribute the lower stress drop for RIS to the hypocentral depth. The mechanics of RIS involve a complex interaction between shear stress, normal stress, and pore pressure (Bell and Nur, 1978; Talwani, 1997a; Chen and Talwani, 2001). After the water filling, under the combined effect due to the load effect and water percolation, the pore pressure increases and the shear stress decreases. Furthermore, the water lubrication may decrease the coefficient of friction and cohesion. Many effects may cause the RIS to occur with lower stress than would happen with more typical tectonic earthquakes.

Conclusions

We investigated a set of 1924 earthquakes (M_L −0.3 to 3.1) recorded by 26 temporary stations from 16 March 2009 to 14 July 2010 in the Three Gorges reservoir area. We found that epicenters are mainly concentrated in three clusters and located along the river within the range of 10 km from reservoir waterfront. The hypocentral depths range from 0 to 15 km and appear to increase with the epicenters approaching the dam.

Source parameters for 97 selected reservoir-induced earthquakes of $M_L \geq 1.5$ were estimated after applying corrections for geometrical spreading, frequency-dependent Q, and site effects. The results show that the seismic moment M_0 ranges from 3.96×10^{11} to 4.07×10^{13} N · m, whereas static stress drops ($\Delta\sigma$) vary from 0.01 to 0.26 MPa. The static stress drop in this area scales with seismic moment as $\Delta\sigma \propto M_0^{0.46}$ for our data range, indicating a departure from constant stress drop scaling down to small earthquakes. We find that apparent stresses also increase with increasing seismic moment over the entire magnitude range. It indicates large earthquakes radiated more energy per seismic moment than small ones in the Three Gorges reservoir area and a large earthquake is a more efficient radiator of seismic energy than are small events.

The compilation results show that reservoir-induced earthquakes in the Three Gorges reservoir area have about ten times lower average stress drop than natural tectonic earthquakes for the magnitude range studied. The low stress drop for RIS indicates it could occur with a lower tectonic stress due to the high pore pressures of the underground medium and the effect of a decrease in the coefficient of friction.

Data and Resources

The data used in this paper were obtained from Portable Digital Seismic Station Network (PDSSN) set up in the Three Gorges reservoir from March 2009 to July 2010 and were proprietary. All of the maps were plotted using Generic Mapping Tools (www.soest.hawaii.edu/gmt, last accessed October 2012; Wessel and Smith, 1998).

Acknowledgments

This research is funded by the National Key Technology R&D Program monitoring and Research Technology of Reservoir Earthquakes (2008BAC38B02) and the Special Research Project in Earthquake Science, China (200808068 and 201208003). This work is also funded by the basic special item for scientific research of Institute of Earthquake Science, China Earthquake Administration (2011TES010104). We thank Bettina P. Allmann for providing us their result data. We are grateful for Chen Hanli who gave us much help in data processing. We thank Associate Editor Cezar I. Trifu and two anonymous reviewers for their careful reviews and valuable comments that helped to improve the manuscript.

References

Abercrombie, R. E. (1995). Earthquake source scaling relationships from −1 to 5 M_L using seismograms recorded at 2.5 km depth, *J. Geophys. Res.* **100,** 24,015–24,036.

Abercrombie, R. E., and P. Leary (1993). Source parameters of small earthquakes recorded at 2.5 km depth, Cajon pass, southern California: Implications for earthquake scaling, *Geophys. Res. Lett.* **20,** 1511–1514.

Allmann, B. P., and P. M. Shearer (2007). Spatial and temporal stress drop variations in small earthquakes near Parkfield, California, *J. Geophys. Res.* **112,** no. B04305, 17, doi: 10.1029/2006JB004395.

Allmann, B. P., and P. M. Shearer (2009). Global variations of stress drop for moderate to large earthquakes, *J. Geophys.Res.* **114,** no. B01310, doi: 10.1029/2008JB005821.

Andrews, D. J. (1986). Objective determination of source parameters and similarity of earthquakes of different size, in *Earthquake Source Mechanics*, S. Das, J. Boatwright, and C. H. Sholtz (Editors), Geophys. Monogr. Ser., Vol. 37, American Geophysical Union, Washington, D. C., 259–268.

Archuleta, R. J. (1986). Downhole recordings of seismic radiation, in *Earthquake Source Mechanics*, S. Das, J. Boatwright, and C. H. Sholtz (Editors), Geophys. Monogr. Ser., Vol. 37, American Geophysical Union, Washington, D. C., 319–330.

Archuleta, R. J., E. Cranswick, C. Mueller, and P. Spudich (1982). Source parameters of the 1980 Mammoth Lakes, California, earthquake sequence, *J. Geophys. Res.* **87,** 4595–4607.

Atkinson, G. M., and R. F. Mereu (1992). The shape of ground motion attenuation curves in Southeastern Canada, *Bull. Seismol. Soc. Am.* **82,** 2014–2031.

Bell, M. L., and A. Nur (1978). Strength changes due to reservoir-induced pore pressure and application to Lake Oroville, *J. Geophys. Res.* **83,** 4469–4483.

Boatwright, J. (1994). Regional propagation characteristics and source parameters of earthquakes in northeastern North America, *Bull. Seismol. Soc. Am.* **84,** 1–15.

Borcherdt, R. D. (1970). Effects of local geology on ground motion near San Francisco Bay, *Bull. Seismol. Soc. Am.* **60,** 29–61.

Brodsky, E. E., and H. Kanamori (2001). Elastohydrodynamic lubrication of faults, *J. Geophys. Res.* **106,** 16,357–16,374.

Brune, J. N. (1970). Tectonic stress and the spectra of seismic waves from earthquakes, *J. Geophys. Res.* **75,** 4997–5009.

Brune, J. N. (1971). Correction, *J. Geophys. Res.* **76,** 5002.

Chael, E. (1987). Spectral scaling of earthquakes in the Miramichi region of New Brunswick, *Bull. Seismol. Soc. Am.* **77,** 347–365.

Chen, L. Y., and P. Talwani (2001). Mechanism of initial seismicity following impoundment of the Monticello reservoir, South Carolina, *Bull. Seismol. Soc. Am.* **91,** 1582–1594.

Di Bona, M., and A. Rovelli (1988). Effects of the bandwidth limitation on stress drops estimated from integrals of the ground motion, *Bull. Seismol. Soc. Am.* **78,** 1818–1825.

Dysart, P. S., J. A. Snoke, and I. S. Sacks (1988). Source parameters and scaling relations for small earthquakes in the Matsushiro region, southwest Honshu, Japan, *Bull. Seismol. Soc. Am.* **78,** 571–579.

Fehler, M. C., and W. S. Phillips (1991). Simultaneous inversion for Q and source parameters of microearthquakes accompanying hydraulic fracturing in granitic rock, *Bull. Seismol. Soc. Am.* **81,** 553–575.

Frankel, A., and H. Kanamori (1983). Determination of rupture duration and stress drop for earthquakes in southern California, *Bull. Seismol. Soc. Am.* **73,** 1527–1551.

Gibowicz, S. J., R. P. Young, S. Talebi, and D. J. Rawlence (1991). Source parameters of seismic events at the Underground Research Laboratory in Manitoba, Canada: Scaling relations for events with moment magnitude smaller than −2, *Bull. Seismol. Soc. Am.* **81,** 1157–1182.

Gupta, H. K. (1992). *Reservoir-Induced Earthquakes*, Elsevier Scientific Publishing Co., Amsterdam, 364 pp.

Gupta, H. K., B. K. Rastogi, and H. Narain (1972a). Common features of the reservoir associated seismic activities, *Bull. Seismol. Soc. Am.* **62,** 481–492.

Gupta, H. K., B. K. Rastogi, and H. Narain (1972b). Some discriminatory characteristics of earthquakes near the Kariba, Kremasta and Koyna artificial lakes, *Bull. Seismol. Soc. Am.* **62,** 493–507.

Hanks, T. C. (1977). Earthquake stress drops, ambient tectonic stresses and stresses that derive plate motions, *Pure Appl. Geophys.* **115,** 441–458.

Hardebeck, J. L., and E. Hauksson (1997). Static stress drop in the 1994 Northridge, California, aftershock sequence, *Bull. Seismol. Soc. Am.* **87,** 1495–1501.

Hartzell, S. (1978). Earthquake aftershocks as Green's functions, *Geophys. Res. Lett.* **5,** 1–4.

Holland, J. H. (1975). *Adaptation in Natural and Artificial Systems*, University of Michigan Press, Ann Arbor, Michigan, 211 pp.

Hough, S. (1996). Observational constraints on earthquake source scaling: Understanding the limits in resolution, *Tectonophysics* **261,** 83–95.

Houston, H. (1990). A comparison of broadband source spectra, seismic energies, and stress drops of the 1989 Loma Prieta and 1988 Armenian earthquakes, *Geophys. Res. Lett.* **17,** 1413–1416.

Hua, W., Z. Chen, and S. Zheng (2009). A study on segmentation characteristics of aftershock source parameters of Wenchuan M 8.0 earthquake in 2008, *Chin. J. Geophys.* **52,** 365–371 (in Chinese with English abstract).

Huang, Y., S. Zheng, J. Liu, X. Zhao, and Y. Kang (2003). Attenuation of ground motion and site response in Guangdong region, *Chin. J. Geophys.* **46,** 54–61 (in Chinese with English abstract).

Humphrey, J., and J. Anderson (1994). Seismic source parameters from the Guerrero subduction zone, *Bull. Seismol. Soc. Am.* **84,** 1754–1769.

Ide, S., and G. C. Beroza (2001). Does apparent stress vary with earthquake size? *Geophys. Res.Lett.* **28,** 3349–3352.

Ide, S., G. C. Beroza, S. G. Prejean, and W. L. Ellsworth (2003). Apparent break in earthquake scaling due to path and site effects on deep borehole recordings, *J. Geophys. Res.* **108,** no. B52271, doi: 10.1029/2001JB001617.

Iwata, T., and K. Irikura (1988). Source parameters of the 1983 Japan earthquake sequence, *J. Phys. Earth* **36,** 155–184.

Izutani, Y., and H. Kanamori (2001). Scale-dependence of seismic energy to moment ratio for strike-slip earthquake in Japan, *Geophys. Res. Lett.* **28,** 4007–4010.

Kanamori, H., and D. L. Anderson (1975). Theoretical basis of some empirical relations in seismology, *Bull. Seismol. Soc. Am.* **65,** 1073–1095.

Kanamori, H., and E. E. Brodsky (2004). The physics of earthquakes, *Rep. Progr. Phys.* **67,** 1429–1496.

Kanamori, H., and L. Rivera (2004). Static and dynamic scaling relations for earthquakes and their implications for rupture speed and stress drop, *Bull. Seismol. Soc. Am.* **94,** 314–319.

Kanamori, H., E. Hauksson, L. K. Hutton, and L. M. Jones (1993). Determination of earthquake energy release and M_L using terrascope, *Bull. Seismol. Soc. Am.* **83,** 330–346.

Kane, D. L., G. A. Prieto, F. L. Vernon, and P. M. Shearer (2011). Quantifying seismic source parameter uncertainties, *Bull. Seismol. Soc. Am.* **101,** 535–543.

Kikuchi, M., and Y. Fukao (1988). Seismic wave energy inferred from long-period body wave inversion, *Bull. Seismol. Soc. Am.* **78,** 1707–1724.

Li, P., Y. J. Li, and M. E. Yang (2005). A study of reservoir-induced earthquake in the Three Gorges area, *Eng. Sci.* **7,** 14–20 (in Chinese with English abstract).

Li, Q., X. Zhao, J. A. Cai, R. F. Liu, G. H. Long, and Y. R. An (2009). P wave velocity structure of upper and middle crust beneath the Three Gorges reservoir dam and adjacent regions, *Sci. China Earth Sci.* **39,** 427–436 (in Chinese with English abstract).

Liao, W. L., L. F. Zhang, and Y. S. Yao (2009). Characteristics of seismicity in the Three Gorges reservoir area, *Seismol. Geol./Di Zhen Di Zhi* **31,** 707–714 (in Chinese with English abstract).

Liu, J., S. Zheng, and Y. Huang (2003). The inversion of anelastic coefficient, source parameters and site respond using genetic algorithm, *Acta Seismol. Sin.* **25,** 211–218 (in Chinese with English abstract).

Ma, W. T., C. P. Xu, J. L. Yuan, H. O. Li, X. W. Xu, X. D. Zhang, and L. F. Zhang (2011). Intensive observation of reservoir-induced seismicity and preliminary analysis on the causes of earthquakes in the Three Gorges reservoir area, Yangtze river, *Earthq. Res. China* **25,** 273–285.

Mandal, P., and U. Dutta (2011). Estimation of earthquake source parameters in the Kachchh seismic zone, Gujarat, India, from strong-motion network data using a generalized inversion technique, *Bull. Seismol. Soc. Am.* **101,** 1719–1731.

Mandal, P., B. K. Rastogi, and C. S. P. Sarma (1998). Source parameters of Koyna earthquakes, India, *Bull. Seismol. Soc. Am.* **88,** 833–842.

Mayeda, K., and W. R. Walter (1996). Moment, energy, stress drop, and source spectra of western United States earthquakes from regional coda envelopes, *J. Geophys. Res.* **101,** 11,195–11,208.

McGarr, A. (1993). Factors influencing the strong ground motion from mining-induced tremors, in *Rockbursts and Seismicity in Mines*, R. P. Young (Editor), Balkema, Rotterdam, 3–12.

Mori, J. (1993). Fault plane determinations for three small earthquakes along the San Jacinto fault, California: Search for cross faults, *J. Geophys. Res.* **98,** 17,711–17,722.

Mori, J., and A. Frankel (1990). Source parameters of aftershocks of the 1986 North Palm Springs earthquake, *Bull. Seismol. Soc. Am.* **80,** 278–295.

Moya, C. A., J. Aguirre, and K. Irikura (2000). Inversion of source parameters and site effects from strong ground motion records using genetic algorithms, *Bull. Seismol. Soc. Am.* **90,** 977–992.

Nuttli, O. W. (1983). Average seismic source-parameter relations for mid-plate earthquakes, *Bull. Seismol. Soc. Am.* **73,** 519–535.

Perez-Campos, X., and G. C. Beroza (2001). An apparent mechanism dependence of radiated seismic energy, *J. Geophys. Res.* **106,** 11,127–11,136.

Prejean, S., and W. L. Ellsworth (2001). Observations of earthquake source parameters at 2 km depth in the Long Valley caldera, eastern California, *Bull. Seismol. Soc. Am.* **91,** 165–177.

Prieto, G. A., P. M. Shearer, F. L. Vernon, and D. Kilb (2004). Earthquake source scaling and self-similarity estimation from stacking *P* and *S* spectra, *J. Geophys. Res.* **109,** no. B08310, doi: 10.1029/2004JB003084.

Roeloffs, E. A. (1988). Fault stability changes induced beneath a reservoir with cyclic variations in water level, *J. Geophys. Res.* **93,** 2107–2124.

Ross, A., G. R. Foulger, and B. R. Julian (1999). Source processes of industrially-induced earthquakes at The Geysers geothermal area, California, *Geophysics* **64,** 1877–1889.

Scholz, C. H. (1990). *The Mechanics of Earthquakes and Faulting*, Cambridge Univ. Press, Cambridge, 439 pp.

Shearer, P. M., G. A. Prieto, and E. Hauksson (2006). Comprehensive analysis of earthquake source spectra in southern California, *J. Geophys. Res.* **111,** no. B06303, doi: 10.1029/2005JB003979.

Sibson, R. (1973). Interactions between temperature and pore-fluid pressure during earthquake faulting and a mechanism for partial or total stress relief, *Nat. Phys. Sci. (Lond.)* **243,** 66–68.

Simpson, D., W. Leith, and C. Scholz (1988). Two types of reservoir-induced seismicity, *Bull. Seismol. Soc. Am.* **78,** 2025–2040.

Singh, S. K., and M. Ordaz (1994). Seismic energy release in Mexican subduction zone earthquakes, *Bull. Seismol. Soc. Am.* **84,** 1533–1550.

Snoke, J. A. (1987). Stable determinations of (Brune) stress drops, *Bull. Seismol. Soc. Am.* **77,** 530–538.

Snoke, J. A., A. T. Linde, and I. S. Sacks (1983). Apparent stress: An estimate of the stress drop, *Bull. Seismol. Soc. Am.* **73,** 339–348.

Snow, D. T. (1972). Geodynamics of seismic reservoirs, *Proc. Sym. Percolation Through Fissured Rock*, Stuttgart, Ges. Erd und Grundbau, T2J, 1–19.

Stork, A. L., and H. Ito (2004). Source parameter scaling for small earthquakes observed at the western Nagano 800-m-deep borehole, central Japan, *Bull. Seismol. Soc. Am.* **94,** 1781–1794.

Tajima, R., and F. Tajima (2007). Seismic scaling relations and aftershock activity from the sequences of the 2004 mid Niigata and the 2005 west off Fukuoka earthquakes (M_w 6.6) in Japan, *J. Geophys. Res.* **112,** no. B10302, doi: 10.1029/2007JB004941.

Talwani, P. (1997a). On the nature of reservoir-induced seismicity, *Pure Appl. Geophys.* **150,** 473–492.

Talwani, P. (1997b). Seismotectonics of the Koyna-Warna area, India, *Pure Appl. Geophys.* **150,** 511–550.

Tomic, J., R. E. Abercrombie, and A. F. do Nascimento (2009). Source parameters and rupture velocity of small M B 2.1 reservoir induced earthquakes, *Geophys. J. Int.* **179,** 1013–1023.

Tusa, G., and S. Gresta (2008). Frequency-dependent attenuation of *P* waves and estimation of earthquake source parameters in southeastern Sicily, Italy, *Bull. Seismol. Soc. Am.* **98,** 2772–2794.

Walter, W. R., K. Mayeda, R. Gok, and A. Hofstetter (2006). The scaling of seismic energy with moment: Simple models compared with observations, in *Earthquakes: Radiated Energy and the Physics of Faulting*, R. Abercrombie, A. McGarr, H. Kanamori, and G. Di Toro (Editors), Geophys. Monogr. Ser., , Vol. 170, AGU, Washington, D. C., pp. 25–41, doi: 10.1029/170GM05.

Wang, W. D. (2009). Strengthening earthquake security project of the Three Gorges reservoir with high-stand of water storage, *Seismol. Geomagn. Observ. Res./Di Zheng Di Ci Guance Yu Yan Jiu* **30,** 36–42 (in Chinese with English abstract).

Wessel, P., and W. H. F. Smith (1998). New, improved version of generic mapping tools released, *Eos Trans. AGU* **79,** no. 47, 579.

Wyss, M., and J. N. Brune (1968). Seismic moment, stress, and source dimensions for earthquakes in the California–Nevada region, *J. Geophys. Res.* **73,** 4681–4694.

Yamada, T., J. J. Mori, S. Ide, H. Kawakata, Y. Iio, and H. Ogasawara (2005). Radiation efficiency and apparent stress of small earthquakes in a South African gold mine, *J. Geophys. Res.* **110,** no. B01305, 18, doi: 10.1029/2004JB003221.

Yang, X. Y., and L. Y. Zhang (2001). Introduction on monitoring system of earthquakes induced by Sanxia reservoir, *Earthq. Res. Sichuan* **99,** 1–5 (in Chinese with English abstract).

Zhao, C., Z. Chen, W. Hua, Q. Wang, Z. Li, and S. Zheng (2011). Study on source parameters of small to moderate earthquakes in the main seismic active regions, China mainland, *Chin. J. Geophys.* **54,** 1478–1489 (in Chinese with English abstract).

Zhou, X., Y. Zhong, J. Fu, F. Yang, and F. Zhang (2006). Contrast of time-frequency characteristics of wave spectrum between Shanxi reservoir induced earthquake and tectonic earthquake, *J. Geod. Geodyn./Dadi Celiang Yu Di Qiou Dong Li Xue* **26,** 86–91 (in Chinese with English abstract).

CEA Key Laboratory of Earthquake Prediction,
Institute of Earthquake Science
China Earthquake Administration
Beijing 100036, China
huawei@seis.ac.cn
(W.H., S.Z., C.Y.)

China Earthquake Administration
Beijing 100036, China
(Z.C.)

Manuscript received 2 March 2012